J Solid State Electrochem (2002) 6: 341–350
DOI 10.1007/s100080100229

ORIGINAL PAPER

Magdy A.M. Ibrahim · Dujreutai Pongkao
Masahiro Yoshimura

The electrochemical behavior and characterization of the anodic oxide film formed on titanium in NaOH solutions

Received: 29 March 2001 / Accepted: 7 June 2001 / Published online: 21 July 2001

Abstract Titanium dissolution and passivation were studied in NaOH aqueous solution using open-circuit potential, potentiodynamic and potentiostatic techniques. Potentiodynamic data showed that the active-passive transition involves active metal dissolution followed by formation of a poorly conducting passive oxide film that passivates the electrode. The critical current density varied with pH as $d \log j_m/dpH = -0.098$ in the pH range 11.00–14.00, while the passivation potential is changed according to the following two features: at pH 10.55–13.00, $dE_m/dpH = -0.06\,V$; and at pH 13.50–14.00, $dE_m/dpH = -0.40\,V$. The apparent activation energy, E^*, was calculated from the slope of the Arrhenius plot and was found to be 12.6 kJ mol^{-1}. Current-time transients showed that the growth of titanium oxide passive film is a diffusion-controlled process. XPS measurements indicated that the passive oxide film consists mainly of TiO_2 and a mixture of suboxides of Ti_2O_3 and TiO.

Keywords Titanium electrode · Passive film · Potentiodynamic data · Open-circuit potential · X-ray photoelectron spectroscopy

Introduction

Titanium and titanium alloys possess good mechanical properties, a high strength-to-weight ratio and excellent corrosion resistance as a result of the native oxide film (~20 Å thick) that spontaneously forms on the surface of the metal in air and aqueous solutions. Hence, they are increasingly used not only for industrial applications [1] but also for medical applications [2]. In recent years, much research [3, 4, 5, 6] has been conducted on different kinds of NaOH-treated titanium substrates for biomaterial applications. Therefore, it is interesting to study the passivation as well as the electrochemical behavior of Ti in NaOH solutions.

Few works have been published on the electrochemical behavior and passivation of Ti in alkaline media [7, 8, 9, 10]. The corrosion behavior of Ti in carbonate-bicarbonate buffer solution of pH 9.7 was studied by El Sayed and Leach [7]. They found that the changes in the impedance and corrosion rate with potential are both due to change of cation valency and to oxide non-stoichiometry. Prusi and Arsov [9] reported the growth kinetics and optical properties of titanium oxide on a Ti surface in KOH solutions under open-circuit potential conditions.

The purpose of the present investigation is to study the passivation behavior of a Ti electrode in NaOH solutions as well as to characterize the passive oxide film. The influence of various parameters, including sweep rate, electrolyte concentration, solution temperature and pH, on the anodic dissolution as well as on the passivation of the Ti electrode was studied.

Experimental

The working electrode employed in the present study was made of pure titanium (99.99%) sheets axially embedded in Araldite holders to offer a Ti exposed surface area of 2.3 cm^2. Prior to each experiment, the working electrode was mechanically polished with different grades of emery paper, i.e., 600, 800, 1000 and finally 1200, and then the polished electrode was rinsed with acetone and distilled water. Finally, the electrode was activated in 1 M HF for 1 min followed by generous washing with double-distilled water, and then dipped in a conventional three-electrode cell. The oxide film was removed when necessary by gentle hand polishing on 0.05 μm alumina. A platinum plate (2.0 cm^2) was used as a counter electrode. All potentials were measured against a Ag/AgCl electrode. To avoid contamination, the reference electrode was connected to the working electrode through a bridge with a Luggin capillary filled with the test solution. The capillary tip was put very close to the electrode surface to minimize the ohmic drop of the

M.A.M. Ibrahim · D. Pongkao · M. Yoshimura (✉)
Center for Materials Design,
Materials and Structures Laboratory,
Tokyo Institute of Technology,
4259 Nagatsuta, Midori-ku,
Yokohama 226-8503, Japan
E-mail: yoshimu1@rlem.titech.ac.jp

solution. Solutions were freshly prepared from doubly distilled water and pure grade chemicals and purged with argon gas for 1 h before the experiment. The electrolyte was exchanged after each measurement in order to avoid build-up of soluble titanium species, which are known to enhance the stability of the oxide under open-circuit conditions. Solutions of different pH values were prepared by mixing 1 M NaOH with appropriate amounts of 5 M H_2SO_4. All measurements were conducted at constant temperature with the help of a water thermostat.

Electrochemical measurements were performed using a potentiostat-galvanostat (EG&G model 273A) connected to a personal computer. Potentiodynamic measurements were carried out by sweeping the potential from –1.5 V to 2.0 V. Potentiostatic anodization was carried out for 1 h at different applied potentials. Potentiostatic current-time transients at constant potentials were recorded in the following way. The Ti electrode was held at the starting potential of –1.5 V for 60 s to attain a reproducible Ti surface, and then the electrode was scanned potentiodynamically from –1.5 V in the positive direction with a sweep rate of 5 mV s^{-1} to a potential limit at which the current-time transients were recorded for 100 s.

X-ray photoelectron spectroscopy (XPS) was carried out using an ESCA-3200 (Shimadzu) operated at a chamber pressure less than 5×10^{-6} Pa, using Mg K_α radiation. The source was run at 6 kV and 30 mA from the magnesium anode. All measurements were conducted at a take-off angle of 45° with respect to the sample surface. The binding energy was calibrated with the line position of the C(1s) peak at 284.6 eV. The surface morphology as well as the thickness of the oxide film was examined using a scanning electron microscope (SEM) (FE-SEM, model S-4500, Hitachi, Tokyo, Japan).

Results and discussion

Open-circuit potential

Titanium electrodes exposed to the atmosphere after mechanical and chemical polishing are covered spontaneously by an oxide film, being predominately titanium dioxide in a dense modification of rutile TiO_2 [10]. As soon as a Ti electrode is immersed in NaOH solutions, at open-circuit conditions, the process of dissolution of the natural oxide film of TiO_2 begins first. Simultaneously, self-passivated film formation also begins. These two processes are recorded on the open-circuit potential (OCP) versus time curves at various concentrations of NaOH, as shown in Fig. 1. The results show that, firstly, the corrosion potential slowly decreased, showing minimum potential values at approximately –1070, –1310 and –1350 mV in 0.5, 1.0 and 2.0 M NaOH, respectively. This could be attributed to the slow dissolution of naturally formed titanium oxide film as mentioned before. After that, the corrosion potential gradually rose to more noble potential values and finally achieved steady-state potential values at approximately –715, –735 and –805 mV in 0.5, 1.0 and 2 M NaOH, respectively, as a result of the self-passivation. The pseudo-like plateau observed at about –1.3 V, when the concentration of NaOH is increased, might be due to the high dissolution power on the Ti oxide. When the solubility product of the oxide is achieved, the potential starts to rise again. It is worth noting that the stronger the NaOH, the longer the time needed to achieve the steady-state potential and the less noble the steady-state potentials, as shown in Fig. 1.

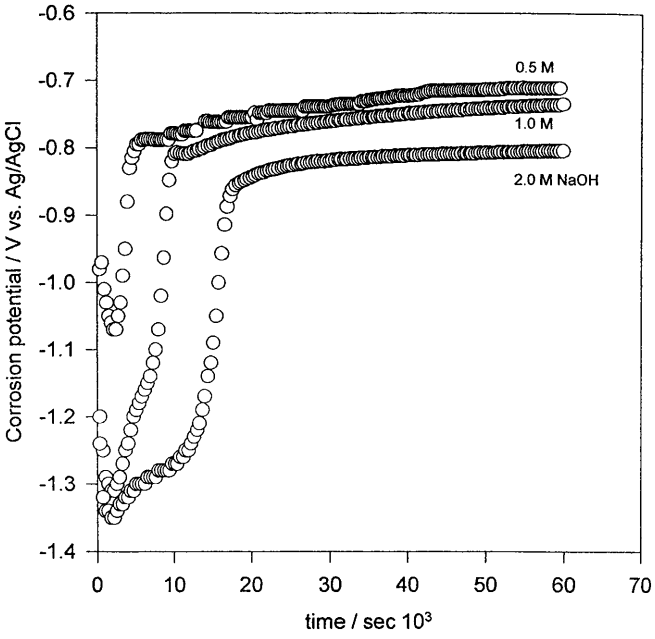

Fig. 1 Corrosion potential versus time of a Ti electrode in different concentrations of NaOH

The open-circuit stability of the passive film in alkaline solution is investigated not only because of its obvious relevance to practical corrosion but also because it allows us to determine the formation rate of the passive film of the Ti electrode. For example, the steady-state potential of the Ti electrode is achieved after 1.9, 2.7 and 6.4 h in 0.5, 1.0 and 2.0 M NaOH, respectively. The broadening in the curve at high NaOH concentrations indicates the competition between dissolution and the formation of the passive oxide film. Generally speaking, the data in Fig. 1 reveal that a shorter time is required for the steady-state potentials to attain in NaOH when compared to the reported data for Ti in acid medium [11].

Potentiodynamic polarization curves

Figures 2, 4, 7 and 10 illustrate the potentiodynamic E/j anodic polarization curves for a Ti electrode in NaOH solution at various NaOH concentrations, pH values, sweep rates and solution temperatures, respectively. The potential sweep was initiated at –1.5 V, where a considerable cathodic current (point a in Fig. 2) is observed and ended at 2.0 V. The cathodic current approaches zero value, and thereafter several characteristic features in the anodic region were observed. These features could be defined as: (1) an active dissolution region between points b and c, where the anodic current increases exponentially with potential; (2) a region where the current increases linearly with potential between c and d; (3) the region of the anodic current peak d; (4) a region in which the anodic current decreases towards a low value, d–e, corresponding to the passivation of the electrode; and (5) the passive range between e and f.

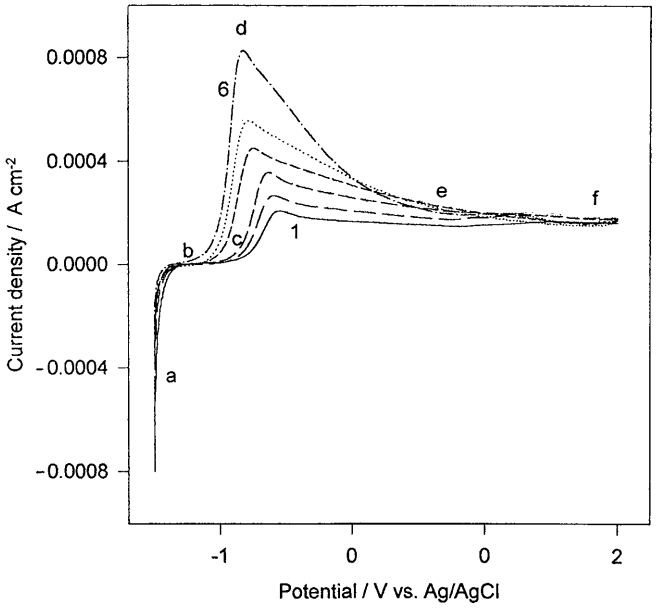

Fig. 2 Potentiodynamic anodic polarization curves of a Ti electrode in various NaOH concentrations at 25 °C and a sweep rate of 10 mV s^{-1}: *curve 1*, 0.1; *curve 2*, 0.5; *curve 3*, 1.0; *curve 4*, 1.5, *curve 5*, 2.0; and *curve 6*, 3.0 M NaOH

As the potential of the Ti electrode is made increasingly positive, the anodic current density rises to a maximum critical value j_m and then decreases as a result of the formation of a protective oxide film, and consequently the metal is transformed from the active to the passive state [12]. The potential at which the critical current density occurred is recorded as the value of the passivation potential E_m [13]. At more positive potentials (region e–f), OH^- ions are discharged on the Ti electrode, and surface layers of a stable oxide are formed (passivity). In this potential region, the rate of Ti dissolution is increasingly hindered and the dissolution rate (i.e., corrosion rate) is independent of potential. Scanning the Ti electrode to 8.0 V in 1 M NaOH solution did not reveal any breakdown potential (not shown). This clearly indicates the thermodynamic stability of the passive film forming spontaneously on the Ti surface [14], consistent with a Pourbaix diagram where solid Ti oxides are thermodynamically stable under such high pH values [12]. The electrode appearance in the passive region was yellowish due to the presence of the anodic oxide film.

It is generally accepted that the mechanism of anodic film growth differs from that of metal deposition. Electro-crystallization of metals is determined completely by the diffusion of metal ions to the surface and the subsequent transfer reactions at the interface. The formation of an anodic film by passivation from NaOH solution requires transfer of titanium and hydroxyl ions as follows:

$$Ti \rightarrow Ti^{2+} + 2e^- \quad (1)$$

Ti^{2+} is unstable and once it is formed it will react with H_2O to produce Ti^{3+}:

$$Ti^{2+} + H_2O \rightarrow Ti^{3+} + OH^- + 0.5H_2 \quad (2)$$

$$Ti^{3+} + 3OH^- \rightarrow Ti(OH)_3 \quad (3)$$

Transformation of $Ti(OH)_3$ might be taking place to a hydrated TiO_2 layer in a dynamic equilibrium reaction as follows:

$$Ti(OH)_3 \rightleftharpoons TiO_2 \cdot H_2O + 0.5H_2 \quad (4)$$

Therefore, the TiO_2 is formed by migration and adsorption of the OH^- ions through the structure defects on the thinnest part of the oxide film. On the other hand, $Ti(OH)_3$ could be transformed to Ti_2O_3 as follows:

$$2Ti(OH)_3 \rightarrow Ti_2O_3 + 3H_2O \quad (5)$$

This suggested mechanism is confirmed (as shown later) by the XPS measurements, which confirm the presence of different Ti valences in the oxide passive film.

Effect of NaOH concentration

The effect of NaOH concentration (0.1–3.0 M) on the potentiodynamic polarization curves of the Ti electrode at 25 °C and a sweep rate of 10 mV s^{-1} was examined and the results are given in Fig. 2. Inspection of the data reveals that the height of the maximum anodic current density j_m is greatly increased and its corresponding potential E_m (passivation potential) is shifted towards more negative (active) potential values at increased NaOH concentration, indicating a high rate of Ti dissolution. Steady-state current densities of 64–92 μA cm^{-2} were achieved within the NaOH concentration range studied, as shown in Table 1. Lower values of steady-state current densities were reported for Ti in acidic medium by Armstrong et al. [15]. The increase in the maximum anodic current density j_m with increased NaOH concentration can be seen from the relation between $\log j_m$ and $\log c_{NaOH}$ in Fig. 3. The relation between $\log i_m$ versus $\log C_{NaOH}$ is not linear and shows two slopes. This behavior seems to indicate the presence of two different mechanisms regarding the effect of NaOH (the chemical passivation and activation effect). The former is the predominant factor in solutions containing NaOH less than 0.75 M (Fig. 3), while the latter is the predominant factor in solutions containing higher concentrations than 0.75 M. The effects caused by increasing NaOH concentration can be interpreted on the basis of enhanced solubilities of Ti oxide on increasing alkali concentration.

Effect of pH

Typical anodic polarization curves for a Ti electrode in 1.0 M NaOH having different pH values ranging from 11.00 to 14.00 are shown in Fig. 4. The curves demonstrate that as the pH increases, j_m increases and E_m

Table 1 Tafel kinetic parameters obtained for a Ti electrode in different NaOH concentrations at 25 °C

NaOH conc. (M)	Tafel slope, b (V decade^{-1})	Exchange current density, j_0 (mA cm^{-2})	Transfer coefficient, α	$R_p \times 10^3$ (Ω cm^2)	Steady-state current density (μA cm^{-2})
0.1	0.27	0.345	0.032	2.88	64
0.2	0.20	0.340	0.043	2.54	67
0.5	0.20	0.338	0.043	2.38	75
1.0	0.20	0.269	0.049	1.43	88
1.5	0.19	1.990	0.049	0.80	92
2.0	0.16	2.991	0.053	0.49	88
3.0	0.16	4.881	0.053	0.25	85

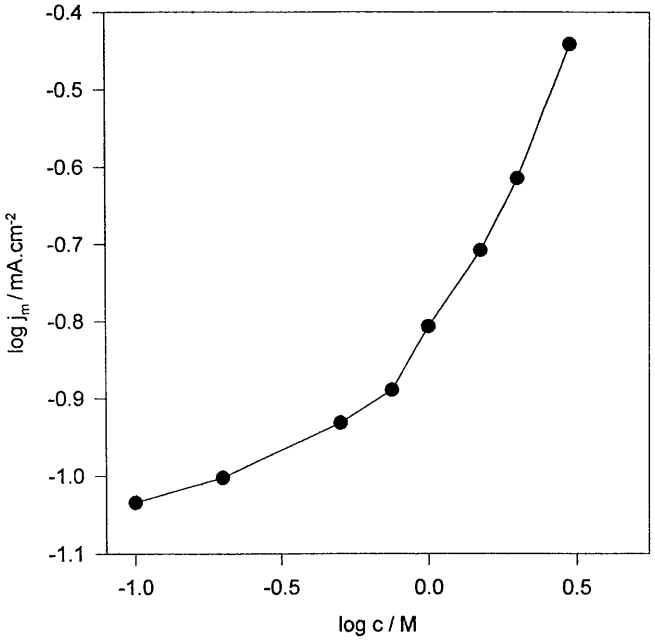

Fig. 3 Dependence of the maximum anodic current density j_m on the concentration of NaOH

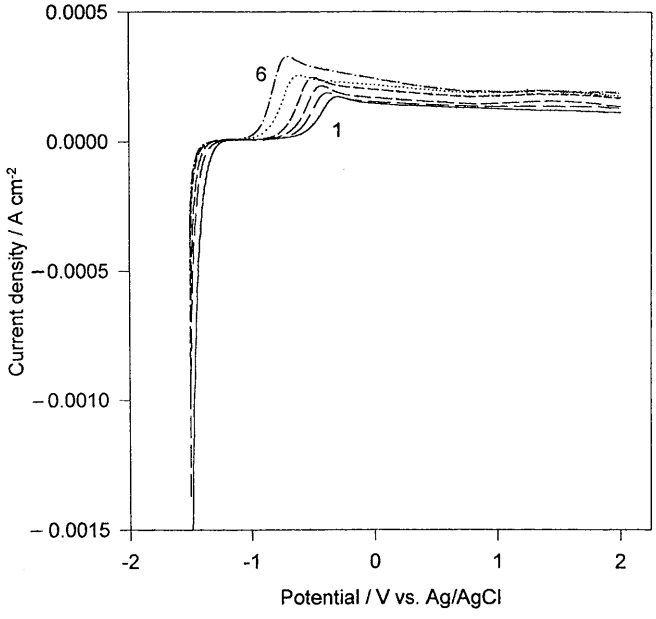

Fig. 4 Potentiodynamic anodic polarization curves of a Ti electrode in 1.0 M NaOH at 25 °C, sweep rate 10 mV s^{-1}, at different pH values: *curve 1*, pH 10.55; *curve 2*, pH 11.50; *curve 3*, pH 12.50; *curve 4*, pH 13.0, *curve 5*, pH 13.25; and *curve 6*, pH 13.50

becomes increasingly negative (active), indicating a high dissolution rate. Moreover, the steady-state current density is increased from about 51 to 85 μA cm^{-2} with increasing pH from 11.00 to 14.00, as shown in Table 2. The steady-state current density was obtained, all through this work, as the current at a potential of +0.8 V. This potential was selected since it was sufficiently noble to permit the formation of a stable passive film.

The relationships between pH and both log j_m and E_m are given in Figs. 5 and 6, respectively, and the data show that, at pH 11.00–14.00, d log j_m/dpH = −0.098; however, for the dependence of E_m on pH it shows two features: at pH 11.00–13.50, dE_m/dpH = −0.06 V; and at pH 13.50–14.00, dE_m/dpH = −0.40 V. Peters and Myers [13] reported a value of d log j_m/dpH = −0.77 and dE_m/dpH = −0.06 V for Ti in sulfuric acid solutions. Such treatment could be useful in establishing quantitative relationships among j_m, E_m and pH. On the other hand, an obvious negative shift for the cathodic reaction was observed with increasing pH (see Fig. 4), revealing the inhibition of the cathodic reaction, which is mainly a hydrogen evolution reaction.

Effect of potential sweep rate

The effect of the potential sweep rate v (2.0–120 mV s^{-1}) on the potentiodynamic polarization responses for a Ti electrode in 1.0 M NaOH at 25 °C was determined and the results are shown in Fig. 7. The data confirm the strong dependence of not only the dissolution rate of Ti but also the growth rate of the oxide film formed on the potential sweep rate. The maximum anodic current density j_m as well as the steady-state current density (Table 3) are dramatically increased with increasing v. On the other hand, the passivating potential E_m is slightly shifted to more positive potentials, as shown from the satisfactory linear fit of E_m versus log v, with a slope of 0.24 s (Fig. 8). The plot of j_m against the square root of v is a straight line passing through origin only at low sweep rates (Fig. 9), in accordance with the following diffusion equation [16]:

$$j_m = abn^{1/2}cD^{1/2}v^{1/2} \quad (6)$$

Table 2 Tafel kinetic parameters obtained for a Ti electrode in 1.0 M NaOH solutions with different pH values at 25 °C

pH	Tafel slope, b (V decade^{-1})	Exchange current density, j_0 (mA cm^{-2})	Transfer coefficient, α	$R_p \times 10^3$ (Ω cm^2)	Steady-state current density(μA cm^{-2})
11.0	0.33	0.160	0.026	4.38	51
12.0	0.33	0.141	0.027	4.30	59
13.0	0.28	0.125	0.031	3.26	62
13.5	0.27	0.121	0.032	2.72	73
13.75	0.26	0.570	0.033	2.50	82
14.0	0.19	0.640	0.049	1.62	85

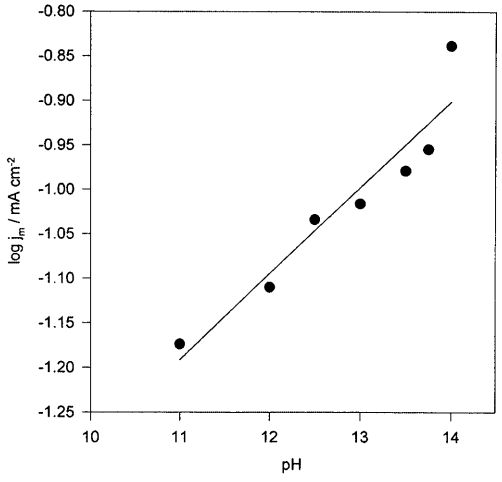

Fig. 5 Dependence of the maximum anodic current density j_m on the pH

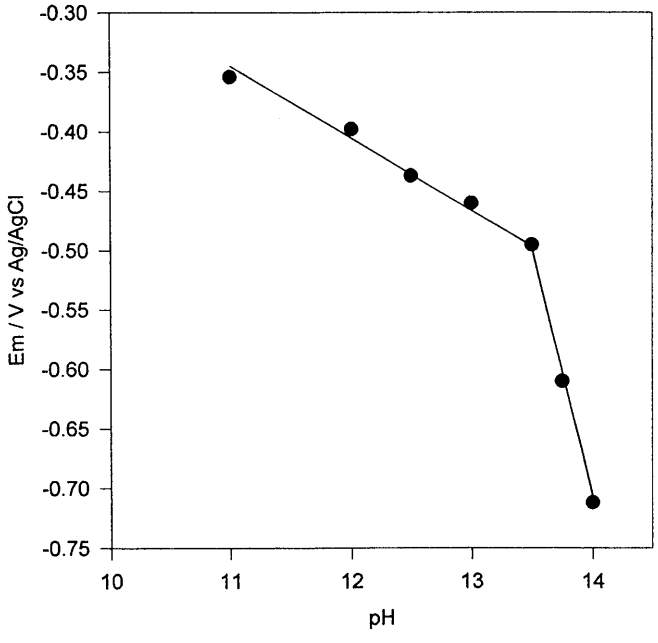

Fig. 6 Dependence of the passivation potential E_m on the pH

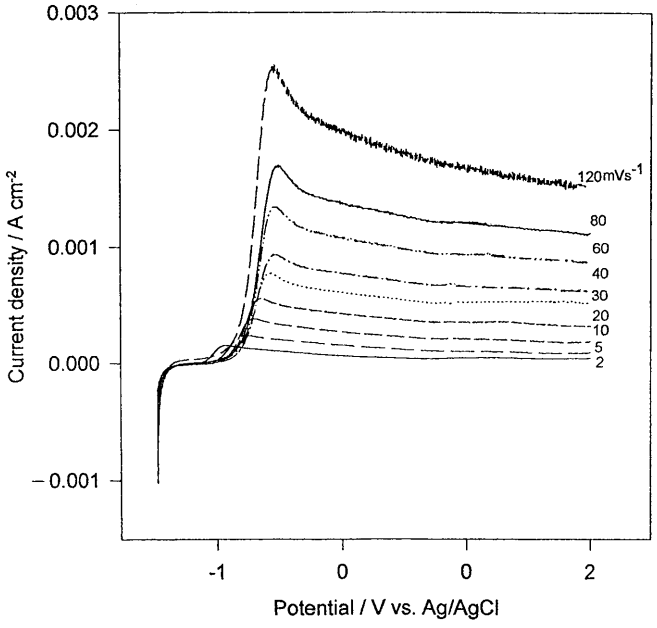

Fig. 7 Potentiodynamic anodic polarization curves of a Ti electrode in 1.0 M NaOH at 25 °C at different sweep rates

where a and b are constants, n is the number of exchanged electrons, c is the concentration, and D is the diffusion coefficients of the diffusing species. This result suggests that the formation of Ti oxide passive layers is a diffusion-controlled process at low sweep rates. However, at high sweep rates, deviations from a straight line are obtained, indicating that the process is not purely diffusion controlled. At low sweep rates, the degree of order in the films increases substantially when they are grown slowly [17]. However, at high sweep rates, the rate of dissolution of the oxide film may compete with the rate of its formation (dissolution-passivation mechanism [18]). Since the time allowed for forming the Ti oxide film becomes shorter as v increases, simultaneous chemical dissolution of Ti oxide is expected. The nature of the oxide film formed at relatively high sweep rates seems different from those formed at relatively low sweep rates, probably due to the fact that the Ti anodic oxide film formed at relatively high sweep rates might have a higher hydration content and OH^- bridges [19]. Consequently, films formed at high sweep rate (more hydrated oxide) are expected to have different properties than those formed at low sweep rates, such as lower density and high dielectric constant. In addition, it was found recently that films formed at different sweep rates present considerably different porosities [20]. It is worthwhile to note that although the sweep rate is one of the most effective parameters affecting the growth rate of

Table 3 Tafel kinetic parameters obtained for a Ti electrode in 1.0 M NaOH with different sweep rates at 25 °C

Sweep rate, v (mV s^{-1})	Tafel slope, b (V $decade^{-1}$)	Exchange current density, j_0 (mA cm^{-2})	Transfer coefficient, α	$R_p \times 10^3$ (Ω cm^2)	Steady-state current density (mA cm^{-2})
2	0.17	5.34	0.050	2.13	0.018
5	0.18	3.49	0.047	1.95	0.044
10	0.18	1.28	0.047	1.31	0.091
20	0.18	1.68	0.045	1.00	0.155
30	0.20	1.79	0.042	0.76	0.225
40	0.20	1.81	0.042	0.64	0.294
60	0.22	1.71	0.038	0.45	0.412
80	0.23	1.52	0.037	0.40	0.523
120	0.24	1.61	0.035	0.22	0.727

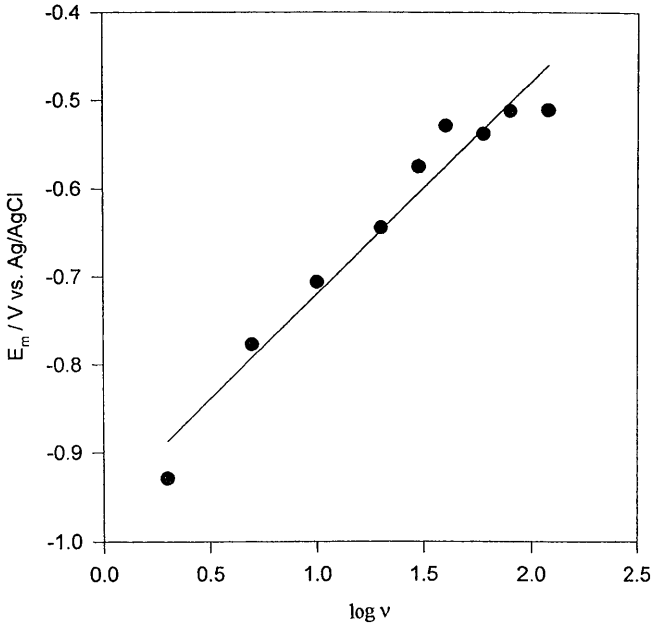

Fig. 8 Dependence of E_m on logarithm of the sweep rate

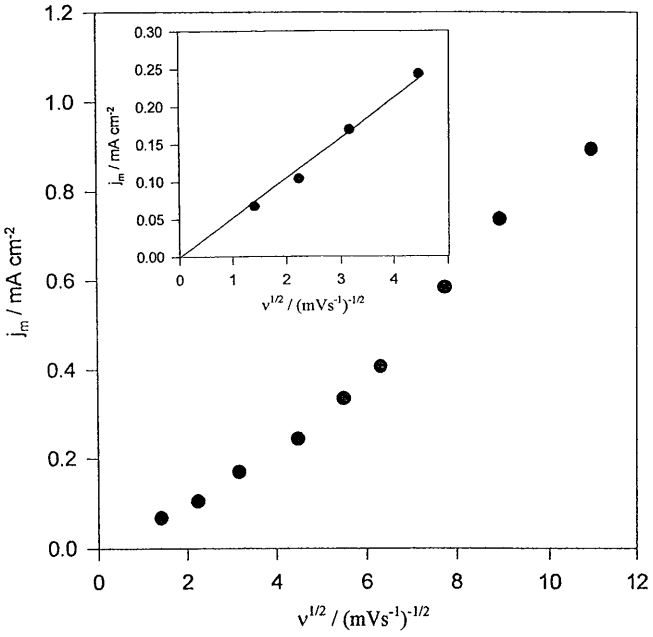

Fig. 9 Dependence of the maximum anodic current density j_m on the square root of the sweep rate of a Ti electrode in 1.0 M NaOH at 25 °C (*insert* is the low sweep rate)

the Ti anodic oxide film and, consequently affecting many other properties, e.g., density, refractive index, dielectric constant and porosity, there is not enough attention given to this topic in the literature.

Effect of temperature

Figure 10 shows the influence of solution temperature on the potentiodynamic anodic polarization curves of a Ti electrode in 1.0 M NaOH at a sweep rate of 10 mV s^{-1}. The rise of solution temperature greatly enhances the critical current density j_m, while the passivating potential E_m is shifted to a more negative potential value. This indicates the high dissolution rate of Ti at higher solution temperatures. In acid medium, E_m is independent of temperature, while j_m is increased with rising temperature [11, 13]. It is obvious that on increasing the solution temperature in the range 35–65 °C, the b–c region in Fig. 2 becomes shorter. However, at temperatures ≥70 °C, the b–c region completely disappears owing to the high dissolution rate of Ti at high temperature. On the other hand, raising the solution temperature has no significant effect on the value of the steady-state current density. The apparent activation energy, E^*, was calculated from the slope of the Arrhenius plot (Fig. 11) according to Eq. 7:

$$j_m = A \exp(-E^*/RT) \tag{7}$$

The data reveal that $\log j_m$ is a function of T^{-1}. The slope, $d \log j_m / d(T^{-1})$, leads to a calculated apparent activation energy of 12.6 kJ mol^{-1}. However, this value is comparatively much lower than that usually reported for Ti in 0.5 M H_2SO_4 [21]. This indicates the high rate of dissolution of Ti in alkaline media in comparison with that in acidic media. The stimulating effect of temperature for the formation of titanium oxide may be attributed to the increase in solubility of the oxides at elevated temperature. In addition, an increase in temperature accelerates the diffusion rate of the diffusing species [22].

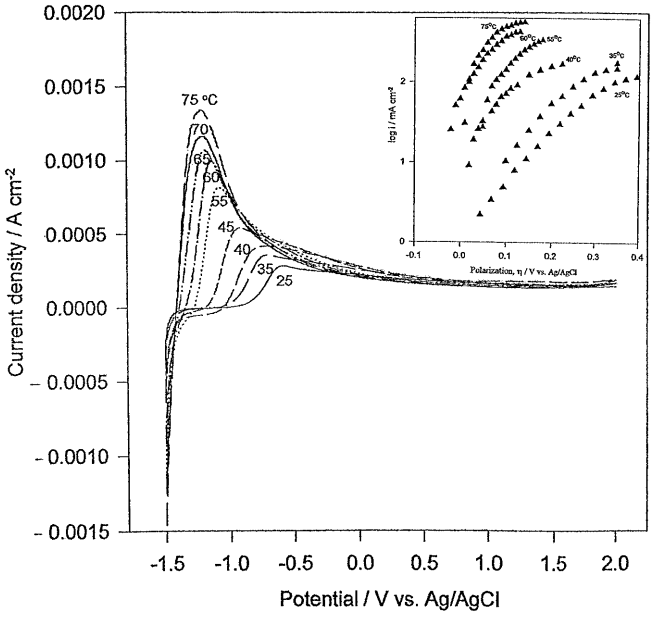

Fig. 10 Potentiodynamic anodic polarization curves and Tafel plots (*insert*) of a Ti electrode in 1.0 M NaOH at 25 °C, sweep rate 10 mV s^{-1}, at different solution temperatures

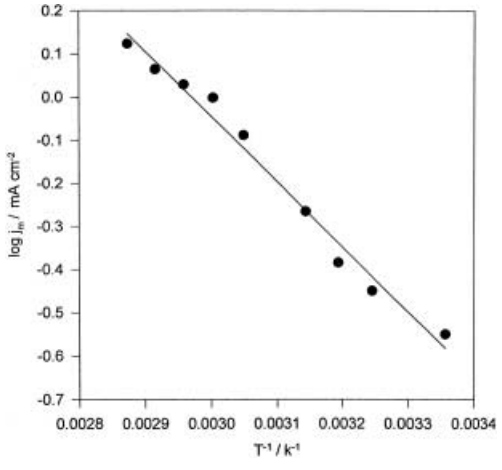

Fig. 11 Dependence of log j_m on T^{-1} (K^{-1}) of a Ti electrode in 1.0 M NaOH

Current transients

In order to gain more information about the electrochemical behavior of Ti in NaOH solutions, potentiostatic current/time transients were recorded. The electrode was first potentiodynamically polarized in the positive direction with a sweep rate of 5 mV s^{-1} to a certain potential (step potential) at which the current-transient was recorded for 100 s. Figure 12 shows the current-time relationship for different anodic step potentials. The transient current decreases monotonically with time to reach a steady-state value. As the anodic step potential is made more positive, the values of the instantaneous and steady-state current increase. At the

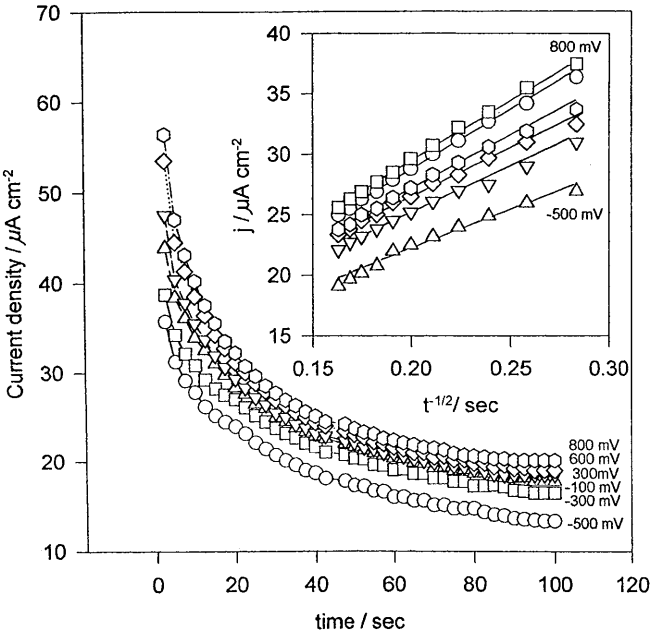

Fig. 12 Current transients versus time recorded in 1.0 M NaOH at 25 °C at constant anodic step potentials (*insert* is the plot of j versus $t^{-1/2}$)

start of each transient there is a charging current that decays during nucleation and initial growth of the surface oxide film followed by a steady-state value (due to the poor conducting effect of the oxide layer formed). Plotting the current density j versus $t^{-1/2}$ for the descending parts of the current transients shows straight lines (Fig. 12 inset). The slopes of the lines depend on the values of the step potentials. This linear relation supports the suggestion that the growth of the Ti oxide layer is a diffusion-controlled process, under this condition, and obeys Eq. 8 [23]:

$$j = P/t^{1/2} \tag{8}$$

where:

$$P = nFcD^{1/2}/\Pi^{1/2} \tag{9}$$

where n is the number of exchanged electrons, c is the concentration and D is the diffusion coefficient of the diffusing species. Therefore, it could be suggested that the formation of Ti anodic oxide film proceeds via metal dissolution followed by a nucleation and growth mechanism under diffusion control.

Tafel kinetic parameters of Ti dissolution

To clarify the effect of NaOH concentration, pH, solution temperature and the sweep rate on the electrode kinetics, Tafel lines are derived from the corresponding *j-E* curves in the active potential regions according to the Tafel equation (Eq. 10):

$$\eta = a - b \log j \tag{10}$$

Table 4 Tafel kinetic parameters obtained for a Ti electrode in 1.0 M NaOH with different solution temperatures

Temperature (°C)	Tafel slope, b (V decade^{-1})	Exchange current density, j_0 (mA cm^{-2})	Transfer coefficient, α	$R_p \times 10^3$ (Ω cm^2)
25	0.18	1.61	0.052	2.09
35	0.18	3.57	0.052	1.58
40	0.16	13.60	0.053	1.20
45	0.16	21.56	0.052	0.77
55	0.16	31.56	0.053	0.34
60	0.15	40.30	0.053	0.34
65	0.15	48.86	0.053	0.34
70	0.15	50.10	0.053	0.25
75	0.15	100.0	0.053	0.23

where:

$$b = -RT/\alpha nF \tag{11}$$

where b is the Tafel slope, α is the transfer coefficient, j is the current density and n is the number of exchanged electrons. Tafel lines are obtained by plotting the logarithm of the current density versus the anodic polarization ($\eta = E - E_r$), where E_r is the equilibrium electrode potential. A representative example for a Tafel plot is given in Fig. 10 (insert); other data are included in Tables 1, 2, 3, 4. The calculated values of Tafel slopes at various conditions of NaOH concentration, pH, sweep rate and solution temperature are also given in Tables 1, 2, 3, 4. The exchange current density, j_0, was obtained by extrapolating the Tafel line to zero overpotential. Moreover, the transfer coefficient, α, and the polarization resistance, R_p (where $R_p = d\eta/dj$ [24]), are also listed in Tables 1, 2, 3, 4. The value of n taken to calculate α is 3.0. It is well known that, in aqueous solution, Ti usually dissolves to Ti^{3+} in the active potential regions [14, 25].

Data in Tables 1, 2, 3, 4 show that the Tafel slope values represented high anomalous Tafel slopes. Experimentally, electrode reactions on oxide-covered electrodes show Tafel slopes greater than 118 mV decade^{-1} [26]. Several attempts have been made to explain these experimental values, the most successful being that of Meyer [27]. The explanations involve the basic assumption that a fraction of the applied overvoltage operates across the oxide and hence is not available to assist the charge transport at the oxide/solution interface. The same assumption may be expressed differently by saying that an activation barrier exists within the oxide film for the transport of electrons through it, and this barrier must be negotiated by the application of a high overvoltage in order for the reaction to occur. Investigation of the data in Tables 1, 2, 3, 4 shows that increasing either the NaOH concentration or the pH gives decreasing values of the Tafel slopes and an increasing effect on the transfer coefficient α, indicating that the charge transfer reaction is affected strongly by increasing any of them [28]. In contrast, increasing the sweep rate has an increasing effect on the Tafel slope and a decreasing effect on α. Generally, the exchange current density value j_0 is increased when the electrochemical reaction is catalyzed [23]. However, the presence of surface oxides, even the most superficial ones, generally results in some deactivation of the electrodes. The deactivation may be defined as a decrease in the exchange current density j_0. Increasing the pH or concentration of NaOH increased j_0 as a result of the high rate of dissolution of the oxide formed, opposite to the effect of increasing the sweep rate. It is worth noting that j_0 is, in general, strongly dependent on temperature, as shown in Table 4 [29]; however, the anodic transfer coefficient α is invariant with temperature [30]. On the other hand, the polarization resistance R_p values decrease with increasing any of the above-mentioned parameters, as shown in Tables 1, 2, 3, 4. High anomalous Tafel slope values ranging from 0.55 to 0.60 V were reported for Ti in alkaline media by Ammar et al. [31]. In acidic media, a Tafel slope of 0.14 V for Ti electrodissolution was estimated by Thomas et al. [24], who suggested the presence of a thin oxide film on the Ti surface in the Tafel region of the hydrogen evolution reaction.

Surface analysis of the passive oxide film using XPS

The Ti($2P_{3/2}$) spectra after potentiostatic oxidation at –0.5 V and 1.2 V in 1 M NaOH for 1 h are shown in Fig. 13. The binding energy of the Ti($2P_{3/2}$) signals was found to be 459 eV. This value is consistent with that reported for TiO_2 [32, 33]. The Ti($2P_{3/2}$) binding energies for TiO_2, Ti_2O_3 and TiO are 459, 457.5 and 455.1 eV, respectively. As shown in Fig. 13, it can be seen that the passive oxide film consists mainly of TiO_2 and suboxides of Ti_2O_3 and TiO. Increasing the potentiostatic potential from –0.5 to 1.2 V (Fig. 13) increases the TiO_2 content in the oxide film. However, the suboxides still coexist with the TiO_2 but are not illuminated, revealing that the oxide passive film consists of mixed oxides. The detected O(1s) signals from the passive oxide film, which are not shown here, are mainly due to the M-O of TiO_2 (530.5 eV). Another small signal of a higher binding energy (531.5 eV) was detected, suggesting the presence of absorbed water and/or OH in the oxide film, as reported by other researchers [33, 34].

A very small amount of sodium ions in the passive film (less than 5%) was detected by quantitative analysis of the XPS measurements. The calibration curve (data not shown) was constructed using TiO_2 (anatase pow-

der) and Na_2CO_3. The pellets of TiO_2 at different molar ratios of Na (in the range 5–95%) were uniaxially pressed, calcined and sintered at 500 °C and 800 °C. The X-ray diffraction pattern of the films formed after potentiostatic oxidation at a potential range from –0.5 V to 2 V cannot show any peaks for rutile or anatase TiO_2. The situation is similar to Raman spectra. No Raman peaks appear, and the structure of the films formed at the above-mentioned potential ranges are amorphous.

Surface morphology

SEM examinations were performed with a series of films prepared potentiostatically at different applied potentials. A representative example is shown in Fig. 14. It is found that changing the applied potentials has no significant effect on the structural morphology or on its thickness, within the potential range studied (0.2–2.0 V). The oxide film is formed in the form of patterns, which is topographical in nature. The thickness (determined by SEM) is thick enough and is about 30 μm.

Conclusion

The electrochemical behavior of a pure titanium electrode in NaOH was studied using open-circuit potential, potentiodynamic and potentiostatic techniques. Potentiodynamic anodic polarization E/j curves show an active-passive transition. The maximum anodic current density j_m increases with increasing NaOH concentration, increasing pH, increasing sweep rate or raising the solution temperature. However, raising the solution temperature, or increasing pH, or increasing the NaOH concentration shows an increasing shifting effect on E_m towards more negative potentials. In contrast, increasing the sweep rate has a reverse effect on E_m, especially at lower sweep rates. The steady-state current density is not significantly affected by raising the solution temperature. However, it is remarkably increased with increasing either the sweep rate or the pH of the solution. The potentiostatic current/time transients show that the

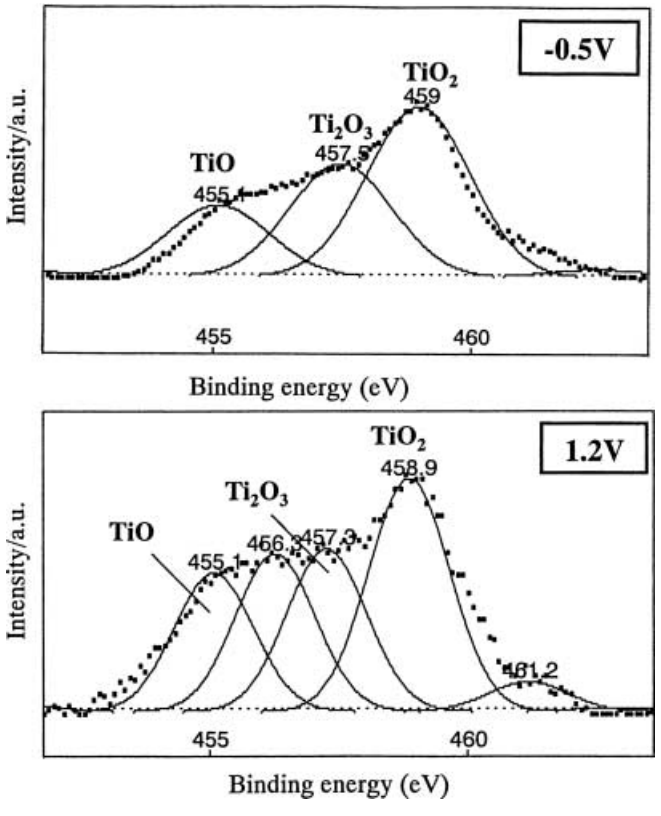

Fig. 13 XPS spectra curve (*dotted line*) for Ti after potentiostatic oxidation at –0.5 V and 1.2 V in 1 M NaOH for 1 h and the deconvoluted curve (*solid line*)

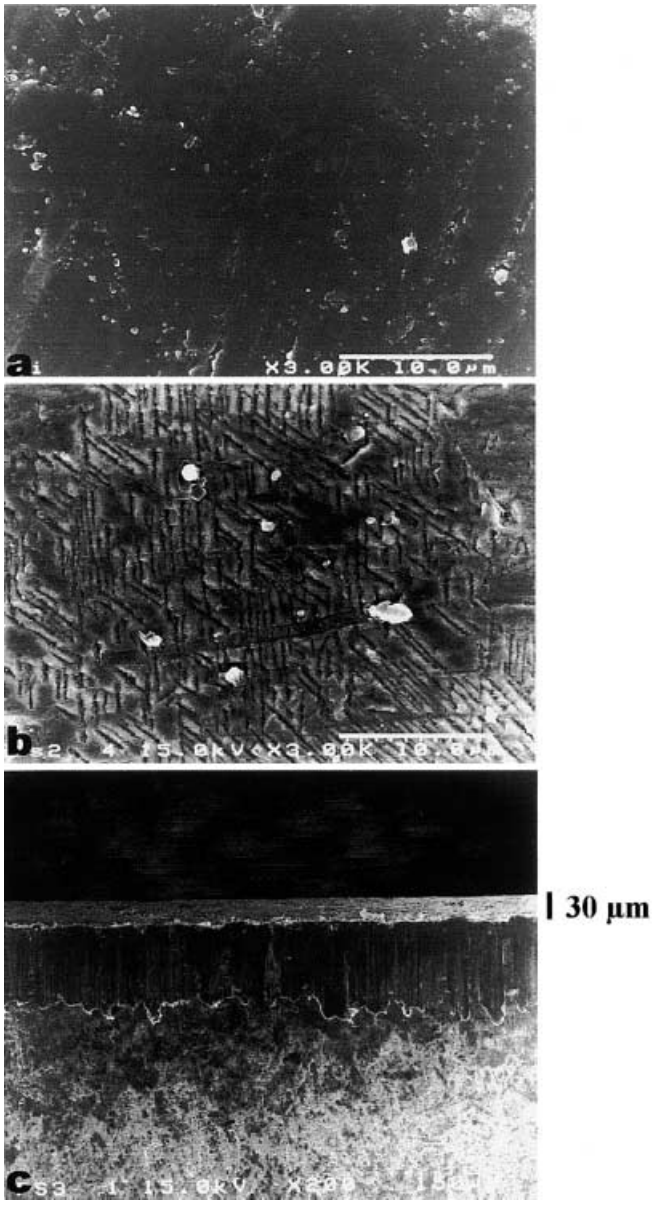

Fig. 14 SEM micrograph of **a** Ti substrate, **b** Ti oxide film potentiostatically formed at 0.2 V in 1.0 M NaOH for 1 h, and **c** cross section of the oxide film formed at 0.2 V in 1.0 M NaOH for 1 h

passive oxide film is formed under a diffusion-controlled process. The apparent activation energy was calculated using an Arrhenius plot and it was found to be 12.6 kJ mol^{-1}. Anomalous high Tafel slopes were obtained in the active potential region. The composition of the passive oxide film consists of TiO_2 and a mixture of suboxides of Ti_2O_3 and TiO, as shown by the XPS data.

Acknowledgements The authors would like to thank Mr. T. Watanabe for experimental assistance with the XPS measurements. This work was supported by JSPS and TJTTP-OECF.

References

1. Seagle SR (1996) Mater Sci Eng A 213:1
2. Mele MFL, Cortizo MC (2000) J Appl Electrochem 30:95
3. Kim H-M, Miyaji F, Kokubo T, Nishiguchi S, Nakamura T (1999) J Biomed Mater Res 45:100
4. Nishiguchi S, Nakamura T, Kobayashi M, Kim H-M, Miyaji F, Kokubo T (1999) Biomaterials 20:491
5. Kim H-M, Miyaji F, Kokubo T, Nakamura T (1997) J Biomed Mater Res 38:121
6. Kim H-M, Miyaji F, Kokubo T, Nakamura T (1996) J Biomed Mater Res 32:409
7. El Sayed AA, Leach JSL (1969) Corros Sci 9: 643
8. Fushimi K, Okawa T, Azumi K, Seo M (2000) J Electrochem Soc 147:524
9. Prusi AR, Arsov LJD (1992) Corros Sci 33:153
10. Blondeau G, Froelicher M, Froment M, Hugot-Le-Goff A, Brieu M, Calsou R, Larroque P (1977) J Microsc Spectrosc Electron 2:27
11. Thomas NT, Nobe K (1969) J Electrochem Soc 116:1748
12. Bard AJ (ed) (1973) Encyclopedia of electrochemistry of the elements. Dekker, New York, pp
13. Peters JM, Myers JR (1967) Corrosion NACE 23:326
14. Armstrong RD, Firman RE (1972) J Electroanal Chem 34:391
15. Armstrong NR, Quinn RK (1977) Surf Sci 67:451
16. Delahy P (1954) New instrumental methods in electrochemistry. Wiley, New York
17. Ohtsuka T, Otsuki T (1998) Corros Sci 40: 951
18. Barrada RG, Belinko K, Ambrose J (1975) Can J Chem 53:389
19. Mandry MJ, Rosenblatt G (1972) J Electrochem Soc 119:29
20. Brunetti V, Villullas HM, Teigels ML (1999) Electrochim Acta 44:4693
21. Kelly EJ (1979) J Electrochem Soc 126:2064
22. Abd El-Rehim SS, Ibrahim MAM, Hassan HH, Amin MA (1998) Can J Chem 76:1156
23. Hamann CH, Hamnett A, Vielstich W (1998) Electrochemistry. Wiley-VCH, New York
24. Thomas NT, Nobe K (1970) J Electrochem Soc 117:622
25. Blackburn MJ, Feeney JA, Beck TR (1973) In: Fontana M, Staehle R (eds) Advances in corrosion science and technology. vol 3. Plenum press, New York, pp 113–
26. Vijh AK (1973) Electrochemistry of metals and semiconductors. Dekker, New York, pp
27. Meyer RE (1960) J Electrochem Soc 107:846
28. Ibrahim MAM (2000) Chem Technol Biotechnol 75:745
29. Tang EZ, Estell TH, Ivey DG (2000) J Electrochem Soc 147:333
30. Bard AJ, Faulkner LR (1980) Electrochemical methods: fundamentals and application. Wiley, New York
31. Ammar IA, Kamal I (1971) Electrochim Acta 16:1555
32. Sayers CN, Armstrong NR (1978) Surf Sci 77:301
33. Nogomi G (1985) J Electrochem Soc 132:76
34. Quinn RK, Armstrong NR (1979) J Electrochem Soc 125:1790